### Title

KRAS oncoprotein expression is regulated by a self-governing eIF5A-PEAK1 feed-forward regulatory loop




### Journal

Cancer Research, 78(6)

### ISSN

0008-5472



### Authors

Fujimura, Ken
Wang, Huawei
Watson, Felicia
et al.



### Publication Date

2018-03-15

### DOI

10.1158/0008-5472.can-17-2873

Peer reviewed

Published in final edited form as:

*Cancer Res*. 2018 March 15; 78(6): 1444–1456. doi:10.1158/0008-5472.CAN-17-2873.

# KRAS oncoprotein expression is regulated by a self-governing eIF5A-PEAK1 feed-forward regulatory loop

**Ken Fujimura**[1,2,#], **Huawei Wang**[1,2,#], **Felicia Watson**[1,2], and **Richard L. Klemke**[1,2]

[1]Department of Pathology, University of California, San Diego, La Jolla, California, 9500 Gilman Drive # 0612, La Jolla, CA 92093

[2]Moores Cancer Center, University of California, San Diego, La Jolla, California, 9500 Gilman Drive # 0612, La Jolla, CA 92093

## Abstract

There remains intense interest in tractable approaches to target or silence the KRAS oncoprotein as a rational therapeutic strategy to attack pancreatic adenocarcinoma (PDAC) and other cancers which overexpress it. Here we provide evidence that accumulation of the KRAS oncoprotein is controlled by a self-regulating feed-forward regulatory loop that utilizes a unique hypusinated isoform of the translation elongation factor eIF5A and the tyrosine kinase PEAK1. Oncogenic activation of KRAS increased eIF5A-PEAK1 translational signaling, which in turn facilitated increased KRAS protein synthesis. Mechanistic investigations shows that this feed-forward positive regulatory pathway was controlled by oncogenic KRAS-driven metabolic demands, operated independently of canonical mTOR signaling, and did not involve new KRas gene transcription. Perturbing eIF5A-PEAK1 signaling, by genetic or pharmacologic strategies or by blocking glutamine synthesis, was sufficient to inhibit expression of KRAS, eIF5A, and PEAK1, attenuate cancer cell growth and migration, and block tumor formation in established preclinical mouse models of PDAC. Levels of KRAS, eIF5A, and PEAK1 protein increased during cancer progression with the highest levels of expression observed in metastatic cell populations. Combinatorial targeting of eIF5A hypusination and the RAS-ERK signaling pathway cooperated to attenuate KRAS expression and its downstream signaling along with cell growth in vitro and tumor formation in vivo. Collectively, our findings highlight a new mechanistic strategy to attenuate KRAS expression as a therapeutic strategy to target PDAC and other human cancers driven by KRAS activation.

### Keywords

eIF5A; KRas; migration; glutamine metabolism; pancreatic cancer

**Corresponding Author:** Richard L. Klemke, School of Medicine, UCSD 9500 Gilman Drive #0612, La Jolla, CA 92093. Phone: 858-822-5610; Fax: 858-822-4566; rklemke@ucsd.edu.

[#]These authors contributed equally to this work

**Conflict of interest statement:** The authors report no conflict of interests.

## Introduction

Eukaryotic translation initiation factor 5A (eIF5A) is an 18-kDa protein that we and others have shown to control cancer cell growth and migration [1–7]. eIF5A is highly conserved from archaea to humans and is essential for normal mammalian development, modulates translation elongation, mRNA transport, and is important for cell-cycle progression as well as proliferation. Emerging evidence indicates that the primary function of eIF5A is not to regulate global protein synthesis, but rather to fine-tune the expression of subsets of proteins required by hyper-proliferating cancer cells, which have significant demands for oncogenic and metabolic proteins. Increased demands for such proteins may explain why eIF5A expression is increased in several cancers, including glioblastoma, leukemia, liver, colon, lung, cervical, ovarian cancer, and pancreatic ductal adenocarcinoma (PDAC) [1–7].

eIF5A's ability to mediate mRNA translation is regulated by a unique posttranslational modification called hypusination [1–7]. Hypusine (N-(4-amino-2-hydroxybutyl)lysine) is formed when deoxyhypusine synthase (DHPS) catalyzes the transfer of the butylamine portion of spermidine to the ε-amino group of a specific lysine substrate of eIF5A (sFig. 1). Carbon 2 of the transferred 4-aminobutyl moiety is then hydroxylated by deoxyhypusine hydroxylase (DOHH). GC7 (N(1)-guanyl-1,7,-diamineoheptane) is an inhibitor of DHPS and DFMO (α-difluoromethylornithine) is an inhibitor of ornithine decarboxylase (ODC), which prevents spermidine synthesis [8–10]. Both drugs inhibit eIF5A hypusination leading to decreased cancer cell growth, differentiation, and metastasis. eIF5A proteins are therefore attractive therapeutic targets for cancer treatment because they are upregulated in proliferating cancer cells, regulate synthesis of cancer-related proteins, and are the only proteins known to be modified by hypusination [11–13].

Our previous work showed that eIF5A1 (eIF5A) is upregulated in human PDAC tissues and in malignant pancreatic cancer tissues isolated from *Pdx-1-Cre: LSL-KRAS*$^{G12D}$mice in a KRas-dependent manner [4, 14–16]. Blocking eIF5A hypusination with GC7 or RNAi-mediated knockdown of eIF5A in PDAC cells inhibited their growth *in vitro* and orthotopic tumor growth *in vivo*, whereas amplification of eIF5A protein increased PDAC cell growth and tumor formation in mice. Hypusinated eIF5A regulates PDAC cell growth by modulating the expression of PEAK1, a tyrosine kinase essential for PDAC cell growth and gemcitabine resistance. PEAK1 is a cytoskeleton-associated nonreceptor tyrosine kinase that plays an essential role in driving PDAC malignancy in cooperation with eIF5A [14, 16]. Like eIF5A, PEAK1 expression is induced by oncogenic KRAS and is amplified in PanINs from *Pdx-1-Cre: LSL-KRAS*$^{G12D}$ mice, and in many PDAC patient tissues samples [14–16]. Blockade of PEAK1 function also inhibits eIF5A expression and prevents PDAC growth and progression. Both eIF5A and PEAK1 expression increase during PDAC cancer progression and are maintained at high levels in metastatic disease. Proteomic analyses of PDAC cells indicated that eIF5A/PEAK1 signaling coordinately regulate cytoskeleton and protein synthesis pathways [14–16]. While eIF5A-PEAK1 signaling is sufficient to drive increased PDAC growth and progression, this process is poorly understood. Here we demonstrate that oncogenic KRas protein expression is controlled by a self-regulating positive feedforward mechanism mediated by eIF5A-PEAK1 signaling. This pathway operates in response to

increased metabolic and energy demands needed to drive KRas-dependent cancer cell proliferation and migration.

## Materials and Methods

### Animals

All animals were treated according to the University of California San Diego animal welfare guidelines as described and approved by the UCSD Institutional Animal Care and Use Committee (S12005).

### Cell lines

The 779E PDAC cell line (obtained from A.M. Lowy, Moores Cancer Center, UCSD, La Jolla CA.) was recently established from a moderate-to-poorly differentiated patient-derived tumor that harbored $KRas^{G12F}$ mutation [14–16]. The 1334 cell line (obtained from A.M. Lowy, Moores Cancer Center, UCSD, La Jolla CA.) was recently established from a PDAC patient liver metastasis and harbors mutated $KRas^{G12D}$ [14–16]. Both of the cell lines were authenticated as PDAC by validating mutations in the KRas gene and by assessing the histology of tumors derived from xenografted lines [14–16]. The FG cell line is a well-differentiated PDAC line that harbors mutated $KRAS^{G12D}$, and was authenticated by assessing cell morphology, the $KRAS^{G12D}$ mutation and cell doubling time, and was kindly provided by Dr. David Cheresh, (Moores Cancer Center, UCSD). The FGM cell line is a highly metastatic variant of FG [15]. PDA4964, PDAA4964-LM, and PDA4313 cells were provided by A.M. Lowy, (Moores Cancer Center, UCSD). Murine PanIN PDA4313 cells were isolated from a mouse PanIN (*Pdx1-cre; LSL-Kras$^{G12D/+}$*). Murine PDA4964 cells were derived from an established primary PDAC tumor (*Pdx1-cre; LSL-Kras$^{G12D/+}$; p53$^{R172H/+}$*), and PDA4964-LM cells were isolated from a matched spontaneous liver metastasis isolated from PDA4964 cells derived from the *Pdx1-cre; LSL-Kras$^{G12D/+}$; p53$^{R172H/+}$* mouse model [14–17]. A549, HPAF-II, PANC1, RD, SW1990, T-24, Colo205, Caco-2, and H1792 cells were obtained from the American Type Tissue Culture Collection (ATCC) between 2008–2017 and have been subcultured for less than 16 passages, and not further authenticated. These cell lines were cultured and passaged according to ATCC recommendations. HPNE, mouse embryonic fibroblast, and human fibroblast cells have been previously described and authenticated [14, 16].

### DNA constructs, viruses, antibodies, and reagents

Antibodies directed at anti-eIF5A (Ab32443), anti-GAPDH (Ab22555), anti-PAN Ras (Ab52939), anti-GLUD1 (Ab55061) were from Abcam. Anti-NRas (Sc-31), Anti-KRas (Sc-30) and anti-HRas (Sc-520) were from Santa Cruz Biotechnology. Anti-HRas (18295–1-AP) was from Proteintech. Anti-PEAK1 (09–274), and the antibody specifically recognizing hypusinated eIF5A (ABS1064) were from Millipore. Anti-c-Myc (#5605), anti-tubulin (#3873), Anti-Erk (#9102) and Anti-P-Erk1/2 to the phosphorylated/activated form of Erk (#9101) were from Cell Signaling. Anti-GOT1 (NBP1–54778) was from Novus.

Constructs encoding shRNAs that target eIF5A1 and eIF5A2 have been previously described and were purchased from Thermo (V3LHS_341459, V3LHS_360415) and Sigma

(TRCN0000062548, TRCN0000147855) [14–16]. Pre-made shRNA lentiviral particles targeting Kras has been previously described and was purchased from Santa Cruz (sc-35731) [15]. The siRNA targeting eIF5A1 was purchased from Thermo (M-015739–00–0005), eIF5A2 and PEAK1 siRNA were from Sigma (SASI_Hs01_00211442 and SASI_Hs02_00357289, respectively). The siRNA targeting KRas was from Qiagen (SI02662051). siRNA to GOT1, HRas, and NRas were from Darmacon. Cell lines stably expressing shRNA eIF5A was generated by puromycin selection (1 μg/ml) after transfection using PEI (Polyethylenimine) or transduction by lentivirus, as described previously [14–16]. Transient transfection was performed by PEI as described previously [14–16]. siRNA transfection was performed using RNAiMAX (Invitrogen) according to the manufacturer's instructions. GFP-PEAK1 gene and control GFP gene were purchased from Sirion Biotech (Germany).

GC7 (N1-guanyl-1, 7-diaminoheptane) was from EMD Millipore, and AOA (aminooxyacetate), EGCG (epigallocatechin gallate), DFMO (α-difluoromethylornithine) were purchased from Sigma. KRasG12C, MEK (AZD6244 and Trametinib) and mTORC1 inhibitors (rapamycin and RAD001) were purchased from Selleck Chemicals.

### GTPase assays

A Ras Activation Assay Kit (ab211159, Abcam) containing RBD Agarose beads was used to pull down and monitor the active RasGTP forms of KRas, NRas and HRas. Subsequently, the precipitated active RasGTP was detected by western blot analyses using anti-KRas, HRas, and NRas antibodies according to the manufacturer's protocol. The ratio of activated GTP to total RAS isoform expression was determined for each sample using densitometry and Image J.

### Migration Assay

Migration was determined as previously described using Corning 8.0 μm porous filters coated with 10 μg/ml fibronection [14–16]. Migrated cells on the lower surface were stained with 0.05% crystal violet, and the number of cells migrated to the lower surface were counted by microscopy. In some cases, normal or dialyzed 10% FBS was placed in the lower chamber as a chemoattractant.

### Quantitative RT-PCR

mRNA extraction, purification, DNA synthesis, and quantitative reverse transcription PCR (qPCR) were performed as described previously [14–16].

### Western blotting

Cell extracts were prepared in RIPA buffer (Cell Signaling Technology) containing complete protease inhibitor cocktail (Roche). Protein concentrations were determined by bicinchoninic acid assay (Pierce). Equal amounts of cell extracts were resolved by SDS-PAGE, transferred to nitrocellulose membranes, and probed with appropriate primary and HRP-conjugated secondary antibodies. Where necessary, membranes were stripped using Restore Western Blot Stripping Buffer (Thermo) and reprobed with a different antibody as previously described [14–16].

### Cell growth, colony forming assays, Gln deprivation, and *in vitro* growth analysis

Clonogenic assays were performed as described previously [14–16]. Briefly, equal number of cells (2500–5000 cells per well) were plated in 24-well plates and subjected to vehicle or drug treatment as indicated. Subsequently, cells were fixed with ice-cold methanol, and stained with 0.05% crystal violet solution. Colony areas of the stained cells were quantified by ImageJ software or the dye eluted with 10% acetic acid and the relative growth determined using spectrophotometry at 595nm. For relative cell growth assays, cells were plated in 24-well plates at 2,000–2500 cells per well. To deprive cells of Gln, cells were first plated in complete culture media (10 mM glucose and 2 mM Gln), which was subsequently exchanged with Gln-free medium supplemented the following day with dialyzed 10% FBS. Cells were allowed to grow for the indicated times then either lysed for western blotting or fixed in methanol and stained with 0.05% crystal violet. The dye was extracted with 10% acetic acid and the relative proliferation determined by spectrophotometry at 595 nm.

### Protein synthesis and degradation assays

Protein synthesis and degradation of KRas and tubulin was determined as previously described [18]. Briefly, subconfluent cells were starved for 24 h in media without methionine. Cells were then supplemented with the same medium with 100 μCi/ml of $^{35}$S-methionine (NEN Life Science Products, Inc.) for 6 h. Cell lysates were immunoprecipitated with anti-KRas antibody (Santa Cruz) and the KRas bands, after autoradiography, were cut out from the membrane and counted in a liquid scintillation counter. For stability determination, cells were starved for 24 h in methionine-free media then supplemented with 100 μCi/ml of $^{35}$S-methionine (NEN Life Science Products, Inc.) for 6 h. After extensive washing, cell lysates were prepared at the indicated times and then immunoprecipitated with an anti-KRas antibody. After autoradiography, the KRas bands were cut from the membrane and counted in a scintillation counter.

### Subcutaneous and orthotopic implantation experiments

Subcutaneous implantation of tumor cells were performed as described previously, by injecting $1\times10^6$ 779E cells to the left flank of 4–6 weeks old female athymic mice [14–16]. Tumors were allowed to grow for 12 days, and subsequently the animals were randomized and subjected to drug administration (GC7, 25mg/kg, daily; and AZD6244, 25mg/kg, every other day). Tumor size was measured using a digital caliper, and tumor volume (V) was calculated using the equation $V = LW^2/2$, where W is width and L is length. Orthotopic implantation experiments were performed essentially as described previously [14–16]. Briefly, 4–6 weeks old female B6/129 mice were anesthetized by intramuscular injection of ketamine, the left lateral flank shaved, and a small incision made through the skin and peritoneum. $1\times10^6$ PDA4964 cells expressing shRNAs were injected into the tail of the pancreas in a total volume of 10 μL of PBS using a Hamilton syringe. The pancreas was returned to the abdomen, and the peritoneum and skin were closed using Polysorb surgical suture. The mice were sacrificed at the indicated time points, and the primary tumor weight was measured.

### Combination index calculation

Combination index (CI) was calculated using Compusyn (Combosyn, Inc.; http://www.combosyn.com/), a freely accessible software that allows calculation of combination index based on the Chou-Talalay method [19]. CI provides quantitative definition for additive effect (CI = 1), synergism (CI < 1), and antagonism (CI > 1) in drug combinations.

### Statistical analysis

All quantified data were plotted and analyzed in GraphPad Prism 6.0 with ANOVA, Student's t-test, or nonlinear regression analysis. Data are representative of at least 3 independent experiments and are reported as mean +/− SD, and * = $P<0.05$, **=$P<0.01$ Student's *t* test.

## Results

### KRas protein expression is controlled by a self-regulating feedforward mechanism mediated by eIF5A-PEAK1

While we previously reported that eIF5A and PEAK1 work cooperatively to drive PDAC growth and migration, the mechanisms are not known. Since KRas mutations are the primary driver in the majority (>90%) of PDAC cases, we investigated the possibility that eIF5A-PEAK1 could regulate KRas expression in a panel of cancer cell lines, which are KRas dependent or independent for cell growth [20] KRas dependency was first confirmed in these cells by shRNA-mediated depletion of KRas (sFig. 2A). Strikingly, 6 of 7 KRas-dependent cell lines and the moderately KRas- dependent cell line PANC1 showed decreased KRas protein expression in response to eIF5A knockdown using two independent shRNAs (Fig. 1A, sFig. 2B). Erk activation was inhibited in the majority (5 of 8) of these cells lines (Fig. 1A). Of the KRas independent cell lines, SW1990 PDAC cells showed no change in KRas expression or Erk activation whereas the lung carcinoma cell line A549 showed reduced KRas expression, but no change in Erk activity upon eIF5A knockdown. Therefore, eIF5A is required for KRas expression and Erk activity in the majority of KRas dependent cancer cell lines, which includes 6 of 7 KRas-dependent PDAC cell lines.

We also examined eIF5A's ability to regulate wild type KRas expression in cancer cell lines as well as normal mouse embryonic fibroblast cells (MEFs). eIF5A depletion did not alter KRas expression in MEFS or two of three cancer cell lines examined (sFig. 2C). These findings suggest that eIF5A does not regulate wild type KRas expression in normal cells, whereas wild type KRas expression in cancer cells is mediated by eIF5A in a context dependent manner. Given the prevalence of KRas in mediating PDAC, we focus here on the role of eIF5A in PDAC cells expressing mutated KRas. Under these conditions depletion of eIF5A or treatment with GC7 or DFMO, which blocks eIF5A hypusination, inhibited KRas expression in PDAC cell lines, and inhibited PDAC tumor cell growth *in vitro* and *in vivo* (Fig. 1A-E, sFig. 2B,D, and E). These findings indicate that hypusinated eIF5A is necessary for proper KRas expression in multiple PDAC cell lines *in vitro* and *in vivo*.

Interestingly, KRas depletion in PDAC cells inhibits eIF5A and PEAK1 protein expression, indicating that eIF5A-PEAK1 expression are also regulated downstream of KRas (Fig. 1F)

[14]. Consistent with these findings, eIF5A or PEAK1 overexpression in PDAC cells increased KRas expression, Erk signaling, and cell growth (Fig. 1G-I). Importantly, siRNA-mediated KRas depletion inhibited eIF5A- and PEAK1-induced PDAC cell growth *in vitro*, indicating this response was mediated by increased KRas expression (Fig. 1H and J). Exogenous expression of eIF5A and PEAK1 together in 779E cells synergistically increased KRas expression levels and cell growth (Fig. 1K). Together these findings indicate that KRas upregulates PEAK1 and eIF5A expression, which in turn, upregulate KRas expression in a positive feedforward loop, to increase PDAC cell growth.

## PEAK1-eIF5A-hypusine signaling is required for $KRas^{G12D}$-induced endogenous NRas and HRas protein expression

KRas activation in tumor cells has been shown to increase expression of endogenous of Ras isoforms (NRas, HRas), which play an important downstream role in growth, migration, chemokine sensing, and DNA damage responses [21, 22]. Therefore, we investigated if KRas-eIF5A-PEAK1 signaling regulated NRas and HRas expression in PDAC cells with activated KRas. HPNE cells are immortalized nestin-positive pancreatic cells commonly used to study transformation and signaling induced by activated KRas [15]. We previously reported that *de novo* expression of $KRas^{G12D}$ in HPNE cells increases PEAK1 and eIF5A expression as well as growth in soft agar [15]. Interestingly, HPNE-$KRas^{G12D}$, but not HPNE cells overexpressing KRas wild type constructs, show increased expression of endogenous HRas and NRas proteins with increased GTPase activity compared to HPNE cells without $KRas^{G12D}$ (Fig. 2A and B). Importantly, KRas knockdown in these cells decreased NRas and HRas expression, indicating that this response was KRas dependent (Fig. 2A, lower panel). siRNA-mediated knockdown of HRas or NRas in HPNE-$KRas^{G12D}$ HPAF-II, and 779E cells significantly inhibited cell growth, indicating that these Ras isoforms are required for mutant KRas-driven PDAC cell growth (Fig. 2C, sFig. 2F). A second antibody (18295-AP) was used to validate HRas expression by western blotting since in some cells anti-HRas antibody sc-520 can react with an unknown 21kD band (Fig. 2C, sFig. 2G) [23]. GC7 treatment and shRNA-mediated depletion of eIF5A in Panc1, 779E, and PDA4964 cells also reduced NRas and HRas expression (Fig. 2D). Importantly, treatment of non-cancerous HUVEC or MEF cells with GC7 inhibited eIF5A hypusination, but did not inhibit cell growth or Ras expression as detected by a pan-Ras antibody (Fig. 2E and F). Together these findings indicate that mutational activation of KRas promotes increased PEAK1-eIF5A signaling, which in turn drives forward increased expression of endogenous HRas and NRas proteins necessary for PDAC cell growth. Interestingly, a PEAK1-eIF5A-mediated feedforward loop may also operate in other Ras-driven cancers. T-24 is a bladder cancer cell line known to be driven by mutated $HRas^{G12V}$ and RD is a rhabdomyosarcoma cell line driven by mutated $NRas^{Q61H}$ [24–26]. shRNA-mediated eIF5A knockdown in these cells inhibited growth and reduced the expression of KRas, NRas, and HRas (Fig. 2G). Conversely, exogenous expression of eIF5A in these cells lines increased KRas, NRas, and HRas expression leading to increased cell growth *in vitro* (Fig. 2H).

## eIF5A-PEAK1 signaling mediates KRas protein synthesis, but not gene transcription

We first investigated whether PEAK1 and eIF5A regulate KRas mRNA expression in PDAC cell lines using qPCR. However, KRas, NRas, HRas mRNA levels as were not significantly

altered in PDAC cells depleted of eIF5A, treated with GC7, or induced to overexpress eIF5A (sFig. 3A-C). Furthermore, HRas and NRas mRNA levels were similar in HPNE-KRas$^{G12D}$ and HPNE cells, and treating HPNE-KRas$^{G12D}$ cells with GC7 did not change Ras mRNA expression levels (sFig. 3 D &E). These findings demonstrate that PEAK1-eIF5A signaling does not regulate KRas, HRas, and NRas gene transcription.

Because PEAK1-eIF5A signaling does not regulate Ras gene transcription, we next investigated whether it regulates protein synthesis of KRas, NRas, and HRas. TORC1 signaling is known to play a critical role in promoting pro-oncogenic protein translation in many cancers [27–29]. The TORC1 signaling cascade is activated by phosphorylated AKT and results in phosphorylation of eIF4E-binding protein (4EBP) and p70S6 kinase (S6K1), which leads to overall mRNA translation [27–29]. To determine whether Ras protein expression is under the control of TORC1, we assessed the effect of rapamycin and its analogue RAD001 on Ras protein expression in PDAC cells [30–32]. Strikingly, even though cells were treated for extended periods of time (72–96 hrs), rapamycin and RAD001 did not significantly inhibit cell growth or KRas, NRas, and HRas expression, whereas it did inhibit S6K1 phosphorylation indicating that TORC1 was inhibited in these cells (sFig. 4A & B). These findings indicate that Ras mRNA translation and protein synthesis are not under control of canonical TORC1 signaling in PDAC cells. In contrast, PDAC cells depleted of eIF5A showed significantly reduced KRas protein synthesis compared to control cells whereas exogenous expression of eIF5A in PDAC cells significantly increased KRas protein synthesis compared to control cells (sFig. 4C and D). The KRas protein degradation rate was similar in control and eIF5A-depleted PDAC cells (sFig. 4E). Furthermore, KRas protein expression and cell growth remained suppressed in eIF5A-depleted cells compared to control cells even after transfection with exogenous KRas$^{G12D}$ (sFig. 4F and G). In fact, there was a greater than 3-fold increase in KRas mRNA, but only a modest increase in KRas protein expression and growth in eIF5A knockdown cells compared to KRas $^{G12D}$ transfected cells (sFig. 4F and G). Considering that exogenous KRas$^{G12D}$ expression in eIF5A knockdown cells further increased endogenous eIF5A protein levels, presumably due to incomplete eIF5A protein depletion (80–90%) and positive feedforward regulation by KRas-eIF5A (Fig 1. G-I), we conclude that eIF5A plays a significant role in regulating KRas protein expression and PDAC cell growth. Together, these findings indicate that eIF5A regulates KRas protein synthesis independent of TORC1 without altering gene transcription and protein degradation.

## Increased KRas-eIF5A-PEAK1 feedforward signaling correlates with cancer progression and metastasis

We previously demonstrated that increased eIF5A and PEAK1 expression correlates with increased cancer progression and metastasis in the KC and KPC mouse models of PDAC, staged human PDAC tissues arrays, and patient cancer databases [14–16]. These findings suggest that KRas-eIF5A-PEAK1 feedforward amplification may contribute to regulation of KRas expression and cancer progression. To investigate this possibility, we used cell lines derived from KC (*Pdx-1-Cre;LSL-Kras$^{G12D/+}$*) and KPC (*LSL-Kras$^{G12D/+}$;LSL-Trp53$^{R172H/+}$;Pdx-1-Cre*) mouse models of PDAC progression [14–17]. PDA4313 (PanIN stage KC-4313), PDA4964 (KPC primary tumor, KPC-4964), and PDA4964-LM cells

(KPC-derived spontaneous liver metastasis, KPC-LM) when transplanted into immune competent hosts faithfully recapitulate the histopathologic steps in human disease progression, including PanIN development, ductal carcinoma, local invasion, and spontaneous metastases to the liver in a highly predictable manner [17]. Using these model cell lines, we found that KRas protein, but not mRNA levels, increase during cancer progression with the highest expression observed in the metastatic KPC-LM cell line (Fig. 3A and B). The increased KRas expression correlated with increased eIF5A and PEAK1 expression (Fig. 3A).

To further investigate KRas expression during malignant progression, we utilized human FG and FGM PDAC cells. FG cells readily form primary tumors in mice, but display low levels of cell migration and metastasis [15]. FGM cells are a highly migratory and metastatic variant derived from FG cells that metastasize to multiple organs including the liver. Consistent with the KC/KPC model of progression, FGM cells show increased KRas, eIF5A, and PEAK1 protein expression compared to parental FG cells (Fig. 3C and D), and treatment with GC7 inhibited KRas protein expression, which decreased cell growth and migration (Fig. 3E-I).

It is interesting that A549 lung carcinoma cells harbor mutationally activated $KRas^{G12S}$, but display KRas-independent growth (Fig. 4A-C) [24–26]. Similarly, SW1990 human PDAC cells harbor mutationally activated $KRas^{G12D}$, but display KRas-independent cell growth (Fig. 4A-C) [24–26]. The role that mutant KRas plays in these cancer cells is not fully understood. Depletion of eIF5A in SW1990 cells did not inhibit KRas expression or growth (Fig. 4A and B). Also, depletion of KRas did not inhibit eIF5A expression or cell growth, indicating that KRas protein expression is not regulated by eIF5A in these cells (Fig. 4A and B). In contrast, depletion of eIF5A in A549 cells strongly decreased KRas expression and siRNA-mediated KRas depletion inhibited eIF5A expression. Consistent with previous reports, KRas depletion did not significantly inhibit A549 cell growth (Fig. 4B and C). These findings indicate that the KRas-eIF5A feedforward signaling operates in A549 cells, but is not required for cell growth. However, KRas is well known to mediate cell migration and cancer metastasis. Interestingly, depletion of eIF5A or KRas in A549, but not SW1990 cells, potently inhibited cell migration (Fig. 4D-G). Together these findings indicate that KRas-eIF5A-PEAK1 feedforward regulation increases during cancer progression where it contributes to cancer cell growth and/or migration.

## Glutamine metabolism regulates KRas-eIF5A-PEAK1 feedforward signaling to mediate cell growth and migration

Cell proliferation and migration increase during cancer progression, which require increased synthesis of proteins needed for energy production, metabolic activities, and cytoskeletal remodeling. Recent work indicates that PDAC cells use glutamine (Gln) to fuel anabolic processes required for energy production, redox balance, and cell growth [33]. Gln deprivation inhibits cell growth and induces cell quiescence [33]. We reasoned that KRas addiction may hijack eIF5A and PEAK1 to maintain Ras expression at a high level to drive forward PDAC cell growth and/or migration. Strikingly, Gln deprivation inhibited PDAC

cell growth, migration, and downregulated expression of KRas, NRas, HRas, eIF5A, and PEAK1 as well as the cell activation markers Erk and c-Myc (Fig. 5A-D).

In many PDAC cells, transaminases are critical for Gln metabolism whereas glutamate dehydrogenase (GLUD1) is dispensable [33]. To determine the role of GLUD1 and transaminases in PDAC cell growth, we treated PDAC cells with the GLUD1 inhibitor epigallocatechin gallate (EGCG) or the pan transaminase inhibitor aminooxyacetate (AOA) [33]. Treatment with AOA, but not EGCG, significantly inhibited PDAC cell growth, migration, and downregulated KRas, NRas, HRas, eIF5A, PEAK1 and c-Myc expression (Fig. 5E-G). In contrast, treatment of normal human fibroblast cells with AOA did not inhibit cell migration, whereas treatment with EGCG did (Fig. 5H). Also, FGM cell migration was more sensitive to AOA treatment than FG cell migration, indicating that they are more dependent on Gln metabolism for cell migration (Fig. 5I). As expected, Gln deprivation did not impact cell growth of A549 or SW1990, which is consistent with the KRas-independent mechanism of growth exhibited by these cells (Fig. 6A and B, Fig. 4B and C). However, A549 cell migration, which is KRas-dependent, was inhibited by Gln deprivation (Fig. 6C). SW1990 cells, which do not require KRas for migration, were not altered by Gln deprivation (Fig. 6C). Consistent with these findings, Gln deprivation inhibited KRas, eIF5A, and PEAK1 expression in A549, but not SW1990 cells (Fig. 6D). Thus, A549 cells use glutamine to fuel cell migration, but not cell proliferation, whereas SW1990 cells do not use Gln for either of these processes. Together these findings indicate that the KRas-eIF5A-PEAK1 feedforward pathway is regulated by transaminase-dependent Gln metabolism which is required for cancer cell growth and migration.

## GOT1 Transaminases are required for PDAC cell proliferation and migration

Cancer cells expressing oncogenic KRas upregulate the expression of a number of metabolic enzymes including proteins involved in Gln metabolism [33]. Of these proteins, the expression of aspartate transaminase GOT1 is increased in a KRas-dependent manner, and is the primary enzyme that regulates Gln metabolism and PDAC cell growth [33]. Depletion of either KRas or eIF5A in A549 cells inhibited GOT1 expression indicating that GOT1 expression is under the control of KRAS-eIF5A signaling in these cells (Fig. 6E). We also observed increased GLUD1 expression which results from reprogramming of Gln-dependent metabolism (Fig. 6E) [33]. In contrast, depletion of either KRas or eIF5A in SW1990 cells did not alter GOT1 or GLUD1 expression, which is consistent with the KRas-independent growth and migration functions of these cells. (Fig. 6F). Furthermore, siRNA-mediated GOT1 knockdown inhibited cell migration, but not proliferation in A549 cells, whereas GOT1 depletion in SW1990 cells failed to inhibit cell migration or proliferation (Fig. 6G and sFig 5A). Also, GOT1 depletion in 779E cells inhibited cell migration and proliferation, which is consistent with their dependency on KRas and Gln metabolism to facilitate these cell functions (Fig. 6H). Together these findings indicate that GOT1-mediated Gln-metabolism is required for cancer cell proliferation and migration.

### Pharmacological inhibition of eIF5A hypusination sensitizes KRas-driven cancer cells to KRas-Erk pathway inhibitors

The ability of hypusinated eIF5A to regulate KRas protein expression provides a unique opportunity to inhibit KRas-driven tumors using pharmacological inhibitors targeting eIF5A and KRas-Erk signaling. Therefore, we investigated whether blockade of eIF5A function would render KRas-mutated tumor cells more vulnerable to specific KRas and Erk pathway inhibitors. As shown in Fig. 7A and B, combined treatment with GC7 and AZD6244, a well characterized MEK inhibitor that is currently in clinical trials, significantly reduced PDAC cell growth, compared to vehicle control and single agent treated cells. We further assessed the synergistic effect of combined treatment with varying doses of GC7 and a constant dose of AZD6244 (1 μM) on PDAC cell growth. For these studies, we calculated the combination index (CI) using the theorem of Chou-Talalay [19]. The drugs synergistically inhibit PDAC cell growth (Fig. 7C, sFig. 5B). Consistent with these findings, combined treatment with DFMO and AZD6244 also synergistically inhibited PDAC cell growth (sFig. 5C).

We next assessed the effect of dual inhibition of eIF5A hypusination and MEK blockade to inhibit PDAC cell growth using subcutaneously grown 779E tumors. While administration of GC7 or AZD6244 as a single agent did reduce tumor growth, combination treatment with both compounds potently suppressed tumor growth without impacting animal viability or body weight (Fig. 7D and E). Western blot analyses of protein lysates from tumors showed GC7 treatment inhibited KRas expression and AZD6244 blocked Erk activation as expected (Fig. 7F). In addition, the combined treatment of DFMO and a KRas-G12C-specific inhibitor potently inhibited growth of H1792 lung adenocarcinoma cells, which harbor KRasG12C (Fig. 7G, sFig. 5D and E) [34]. Altogether, our data indicate that combination therapy targeting eIF5A hypusination and Ras-Erk signaling is a potential strategy to combat KRas-driven tumors. However, additional long-term tumor growth, resistance, and animal health studies are warranted before the efficacy of targeting this pathway can be truly determined.

## Discussion

Our findings uncover a unique feedforward mechanism whereby oncogenic KRas can modulate its own expression level in PDAC cells by hijacking eIF5A-PEAK1-mediated translation. This feedforward mechanism modulates KRas expression according to metabolic and energy demands required for PDAC cell proliferation and migration (sFig. 6). PDAC cells addicted to activated KRas may have evolved a self-adjusting mechanism to maintain optimal levels of KRas to avoid cell senescence, while supporting cell growth, metabolism, and migration (sFig. 6). Indeed, KRas, eIF5A, and PEAK1 levels increase during PDAC progression and are elevated in highly metastatic cell variants. Furthermore, eIF5A and PEAK1 expression increase during PDAC cancer progression and correlate with patient outcome [14]. In addition, a KRas self-regulating mechanism may be important for controlling the total threshold of Ras signaling output in cells. Our findings show that KRas-eIF5A-PEAK1 signaling controls NRas and HRas expression, which are required for PDAC cell growth.

Interestingly, a PEAK1-eIF5A-mediated feedforward loop may also operate in other cancers driven by mutated Ras family members including oncogenic HRas and NRas (Figure 2G-H). Our findings support the emerging idea that oncogenic Ras signaling output itself is not just a simple on-off binary switch, but rather is the sum population of Ras molecules in a cell that act in concert, much like a rheostat, to modulate signal strength and output. Total Ras (KRas, HRas, NRas) protein abundancy has been shown to be a contributing factor in determining oncogenic potency in PDAC and other cancers, but the mechanisms that mediate this response are not understood [35–37]. In addition, extracellular factors from the tumor stroma can further drive Ras signaling to promote cancer development and disease progression [36]. Our findings support the notion that KRas protein expression levels are modulated in response to changes in extracellular Gln. These findings indicate that normal and oncogenic Ras proteins are much more plastic than originally thought, and can self–adjust their expression levels according to the demands of the cell and/or extracellular environment.

Our work supports emerging data that KRas mRNA translation is uniquely regulated due to structural constraints. For example, KRas possesses G-quadruplex motifs in the 5′UTR, which complicates the assembly of the translation initiation machinery at the 5′ cap of the mRNA and can perturb ribosome scanning of start codons [38–41]. As its name implies, eukaryotic translation initiation Factor 5 (eIF5A) has been implicated in regulating translation initiation and, thus could play a novel role in KRas mRNA translation initiation by alleviating the natural structural constraints imposed by G-quadruplex structures at the ribosome mRNA interface [2, 3, 5–7]. Also, rare codon usage reduces efficiency of translation elongation, and KRas is unusually enriched for rare codons [42]. As eIF5A has been shown to increase elongation efficiency, it is conceivable that eIF5A could relieve inefficiencies of KRas translation elongation due to rare codon usage. In addition, eIF5A's ability to travel to the nucleus, bind RNA, and selectively export specific mRNAs to the cytoplasm in a hypusine-dependent manner could provide another level of KRas regulation [43–47]. Thus, KRas translation is uniquely complex and additional mechanistic work is warranted to determine eIF5A's precise role in this process.

Recent work indicates that Gln and GOT1/GOT2 transaminases are uniquely utilized by KRas to fuel anabolic processes necessary for PDAC cell growth [33]. Similarly, we found that KRas-dependent PDAC cells deprived of Gln are static and do not grow. However, we also discovered that PDAC cells require Gln metabolism for cell migration. While it is generally appreciated that cancer cell movement is an energy demanding process, the metabolic mechanisms responsible are not well defined, especially in PDAC, which is characterized by highly invasive and metastatic properties. Previous work showed that inhibiting mitochondria function reduces cell invasiveness whereas pyruvate metabolism increases cell invasion [48]. Gln metabolism has been shown to be a key mitochondrial substrate driving ovarian cancer migration, invasion, and metastasis [48]. Our findings show that Gln metabolism is also a key metabolic process mediating PDAC cell migration which is regulated by KRas-eIF5A-PEAK1 feedforward signaling. Gln deprivation, pharmacological inhibition of transaminases, or GOT1 knockdown in PDAC or A549 lung cancer cells blocked cell migration and reduced KRas-eIF5A-PEAK1 expression. Also, highly metastatic FGM cells showed increased KRas-eIF5A-PEAK1 expression and were

more sensitive to transaminase inhibition by AOA compared to low metastatic FG cells. These findings suggest that metastatic cells may be more dependent on Gln metabolism and energy production, most likely due to their hyperactive cell migration machinery.

Possible clinical applications of our work are based on the fact that DFMO and GC7 attenuate oncogenic, but not wild type Kras protein in PDAC. DFMO is an FDA approved drug to treat African trypanosomiasis and excessive facial hair growth in women [8–10, 49]. DFMO inhibits ODC activity, polyamine biosynthesis, and spermidine production, which is necessary for eIF5A hypusination. Importantly, recent work showed that ODC levels and polyamine biosynthesis are increased in PDAC, and that treating $p48^{Cre/+}$-LSL-$KRas^{G12D/+}$ mice with DFMO inhibits PDAC development and progression [49]. Furthermore, our findings demonstrate that DFMO and GC7 can each inhibit eIF5A hypusination effectively attenuating the KRas-induced feedforward expression and PDAC cell growth. Even more important, we found that downregulation of KRas expression by DFMO or GC7 substantially increased the susceptibility of KRas-driven PDAC cells to inhibitors targeting Ras-Erk signaling. In fact, *in vitro* growth assays indicate that DFMO and GC7 work synergistically with the Ras-Erk pathway inhibitors to prevent PDAC cell growth. These findings suggest that targeting both the hypusine pathway and KRas-Erk signaling could provide a unique mechanism to treat PDAC in the clinic. DFMO could be readily repositioned for PDAC, and several Ras-Erk pathway inhibitors are available or being developed for the clinic.

## Supplementary Material

Refer to Web version on PubMed Central for supplementary material.

## Acknowledgments

The authors thank Dr. David Cheresh (UCSD) for kindly providing the FG and FGM cell lines. We would like to thank Dr. Andrew Lowy (UCSD, Moores Cancer Center) for kindly providing 779E, PDA4964, PDAA4964-LM, and PDA4313. This work was supported by funding from NIH to R.L.K (CA182495 and CA097022), from NCI to K.F (CA180374).

**Financial support:** This work was supported by the NIH-F32 Postdoctoral Fellowship F32CA180374 (K. Fujimura) and NIH grants CA097022 and CA182495 (R.L. Klemke).

## References

1. Wang FW, Guan XY, Xie D. Roles of eukaryotic initiation factor 5A2 in human cancer. Int J Biol Sci. 2013; 9(10):1013–20. [PubMed: 24250246]
2. Dever TE, Gutierrez E, Shin BS. The hypusine-containing translation factor eIF5A. Crit Rev Biochem Mol Biol. 2014; 49(5):413–25. [PubMed: 25029904]
3. Rossi D, et al. eIF5A and EF-P: two unique translation factors are now traveling the same road. Wiley Interdiscip Rev RNA. 2014; 5(2):209–22. [PubMed: 24402910]
4. Fujimura K, et al. Eukaryotic Translation Initiation Factor 5A (EIF5A) Regulates Pancreatic Cancer Metastasis by Modulating RhoA and Rho-associated Kinase (ROCK) Protein Expression Levels. J Biol Chem. 2015; 290(50):29907–19. [PubMed: 26483550]
5. Mathews MB, Hershey JW. The translation factor eIF5A and human cancer. Biochim Biophys Acta. 2015; 1849(7):836–44. [PubMed: 25979826]

6. Caceres CJ, et al. Targeting deoxyhypusine hydroxylase activity impairs cap-independent translation initiation driven by the 5′untranslated region of the HIV-1, HTLV-1, and MMTV mRNAs. Antiviral Res. 2016; 134:192–206. [PubMed: 27633452]
7. Buskirk AR, Green R. Ribosome pausing, arrest and rescue in bacteria and eukaryotes. Philos Trans R Soc Lond B Biol Sci. 2017; 372(1716)
8. Jasiulionis MG, et al. Inhibition of eukaryotic translation initiation factor 5A (eIF5A) hypusination impairs melanoma growth. Cell Biochem Funct. 2007; 25(1):109–14. [PubMed: 16850525]
9. Nakanishi S, Cleveland JL. Targeting the polyamine-hypusine circuit for the prevention and treatment of cancer. Amino Acids. 2016; 48(10):2353–62. [PubMed: 27357307]
10. Shi XP, et al. Effects of N1-guanyl-1,7-diaminoheptane, an inhibitor of deoxyhypusine synthase, on the growth of tumorigenic cell lines in culture. Biochim Biophys Acta. 1996; 1310(1):119–26. [PubMed: 9244184]
11. Carlson-Banning KM, et al. Toward repurposing ciclopirox as an antibiotic against drug-resistant Acinetobacter baumannii, Escherichia coli, and Klebsiella pneumoniae. PLoS One. 2013; 8(7):e69646. [PubMed: 23936064]
12. Sallman DA, Lancet JE. What are the most promising new agents in acute myeloid leukemia? Curr Opin Hematol. 2017; 24(2):99–107. [PubMed: 28030373]
13. Stein EM, Tallman MS. Emerging therapeutic drugs for AML. Blood. 2016; 127(1):71–8. [PubMed: 26660428]
14. Fujimura K, et al. A hypusine-eIF5A-PEAK1 switch regulates the pathogenesis of pancreatic cancer. Cancer Res. 2014; 74(22):6671–81. [PubMed: 25261239]
15. Kelber JA, et al. KRas induces a Src/PEAK1/ErbB2 kinase amplification loop that drives metastatic growth and therapy resistance in pancreatic cancer. Cancer Res. 2012; 72(10):2554–64. [PubMed: 22589274]
16. Strnadel J, et al. eIF5A-PEAK1 Signaling Regulates YAP1/TAZ Protein Expression and Pancreatic Cancer Cell Growth. Cancer Res. 2017; 77(8):1997–2007. [PubMed: 28381547]
17. Hingorani SR, et al. Trp53R172H and KrasG12D cooperate to promote chromosomal instability and widely metastatic pancreatic ductal adenocarcinoma in mice. Cancer Cell. 2005; 7(5):469–83. [PubMed: 15894267]
18. Gatzka M, Prisco M, Baserga R. Stabilization of the Ras oncoprotein by the insulin-like growth factor 1 receptor during anchorage-independent growth. Cancer Res. 2000; 60(15):4222–30. [PubMed: 10945634]
19. Chou TC. Drug combination studies and their synergy quantification using the Chou-Talalay method. Cancer Res. 2010; 70(2):440–6. [PubMed: 20068163]
20. Deer EL, et al. Phenotype and genotype of pancreatic cancer cell lines. Pancreas. 2010; 39(4):425–35. [PubMed: 20418756]
21. Grabocka E, Commisso C, Bar-Sagi D. Molecular pathways: targeting the dependence of mutant RAS cancers on the DNA damage response. Clin Cancer Res. 2015; 21(6):1243–7. [PubMed: 25424849]
22. Grabocka E, et al. Wild-type H- and N-Ras promote mutant K-Ras-driven tumorigenesis by modulating the DNA damage response. Cancer Cell. 2014; 25(2):243–56. [PubMed: 24525237]
23. Waters AM, et al. Evaluation of the selectivity and sensitivity of isoform- and mutation-specific RAS antibodies. Sci Signal. 2017; 10(498)
24. Kovnat A, et al. Malignant properties of sublines selected from a human bladder cancer cell line that contains an activated c-Ha-ras oncogene. Cancer Res. 1988; 48(17):4993–5000. [PubMed: 3409229]
25. Huang HJ, et al. MiR-214 and N-ras regulatory loop suppresses rhabdomyosarcoma cell growth and xenograft tumorigenesis. Oncotarget. 2014; 5(8):2161–75. [PubMed: 24811402]
26. Martinelli S, et al. RAS signaling dysregulation in human embryonal Rhabdomyosarcoma. Genes Chromosomes Cancer. 2009; 48(11):975–82. [PubMed: 19681119]
27. Ebrahimi S, et al. Targeting the Akt/PI3K signaling pathway as a potential therapeutic strategy for the treatment of Pancreatic Cancer. Curr Med Chem. 2017

28. Iriana S, et al. Targeting mTOR in Pancreatic Ductal Adenocarcinoma. Front Oncol. 2016; 6:99. [PubMed: 27200288]
29. Soliman GA, Steenson SM, Etekpo AH. Effects of Metformin and a Mammalian Target of Rapamycin (mTOR) ATP-Competitive Inhibitor on Targeted Metabolomics in Pancreatic Cancer Cell Line. Metabolomics (Los Angel). 2016; 6(3)
30. Brotelle T, Bay JO. [PI3K-AKT-mTOR pathway: Description, therapeutic development, resistance, predictive/prognostic biomarkers and therapeutic applications for cancer]. Bull Cancer. 2016; 103(1):18–29. [PubMed: 26582734]
31. Gu G, Dustin D, Fuqua SA. Targeted therapy for breast cancer and molecular mechanisms of resistance to treatment. Curr Opin Pharmacol. 2016; 31:97–103. [PubMed: 27883943]
32. Porta C, Paglino C, Mosca A. Targeting PI3K/Akt/mTOR Signaling in Cancer. Front Oncol. 2014; 4:64. [PubMed: 24782981]
33. Zheng Y, et al. Temporal regulation of EGF signalling networks by the scaffold protein Shc1. Nature. 2013; 499(7457):166–71. [PubMed: 23846654]
34. Ostrem JM, et al. K-Ras(G12C) inhibitors allosterically control GTP affinity and effector interactions. Nature. 2013; 503(7477):548–51. [PubMed: 24256730]
35. Omerovic J, et al. Ras isoform abundance and signalling in human cancer cell lines. Oncogene. 2008; 27(19):2754–62. [PubMed: 17998936]
36. di Magliano MP, Logsdon CD. Roles for KRAS in pancreatic tumor development and progression. Gastroenterology. 2013; 144(6):1220–9. [PubMed: 23622131]
37. Mageean CJ, et al. Absolute Quantification of Endogenous Ras Isoform Abundance. PLoS One. 2015; 10(11):e0142674. [PubMed: 26560143]
38. Balasubramanian S, Hurley LH, Neidle S. Targeting G-quadruplexes in gene promoters: a novel anticancer strategy? Nat Rev Drug Discov. 2011; 10(4):261–75. [PubMed: 21455236]
39. Neidle S. A Personal History of Quadruplex-Small Molecule Targeting. Chem Rec. 2015; 15(4): 691–710. [PubMed: 26096791]
40. Ohnmacht SA, et al. A G-quadruplex-binding compound showing anti-tumour activity in an in vivo model for pancreatic cancer. Sci Rep. 2015; 5:11385. [PubMed: 26077929]
41. Ohnmacht SA, Neidle S. Small-molecule quadruplex-targeted drug discovery. Bioorg Med Chem Lett. 2014; 24(12):2602–12. [PubMed: 24814531]
42. Pershing NL, et al. Rare codons capacitate Kras-driven de novo tumorigenesis. J Clin Invest. 2015; 125(1):222–33. [PubMed: 25437878]
43. Lee SB, et al. The effect of hypusine modification on the intracellular localization of eIF5A. Biochem Biophys Res Commun. 2009; 383(4):497–502. [PubMed: 19379712]
44. Parreiras ESLT, et al. The N-terminal region of eukaryotic translation initiation factor 5A signals to nuclear localization of the protein. Biochem Biophys Res Commun. 2007; 362(2):393–8. [PubMed: 17707773]
45. Taylor CA, et al. Eukaryotic translation initiation factor 5A induces apoptosis in colon cancer cells and associates with the nucleus in response to tumour necrosis factor alpha signalling. Exp Cell Res. 2007; 313(3):437–49. [PubMed: 17187778]
46. Jao DL, Yu Chen K. Subcellular localization of the hypusine-containing eukaryotic initiation factor 5A by immunofluorescent staining and green fluorescent protein tagging. J Cell Biochem. 2002; 86(3):590–600. [PubMed: 12210765]
47. Trifillis P, Day N, Kiledjian M. Finding the right RNA: identification of cellular mRNA substrates for RNA-binding proteins. RNA. 1999; 5(8):1071–82. [PubMed: 10445881]
48. Yang L, et al. Metabolic shifts toward glutamine regulate tumor growth, invasion and bioenergetics in ovarian cancer. Mol Syst Biol. 2014; 10:728. [PubMed: 24799285]
49. Mohammed A, et al. Eflornithine (DFMO) prevents progression of pancreatic cancer by modulating ornithine decarboxylase signaling. Cancer Prev Res (Phila). 2014; 7(12):1198–209. [PubMed: 25248858]

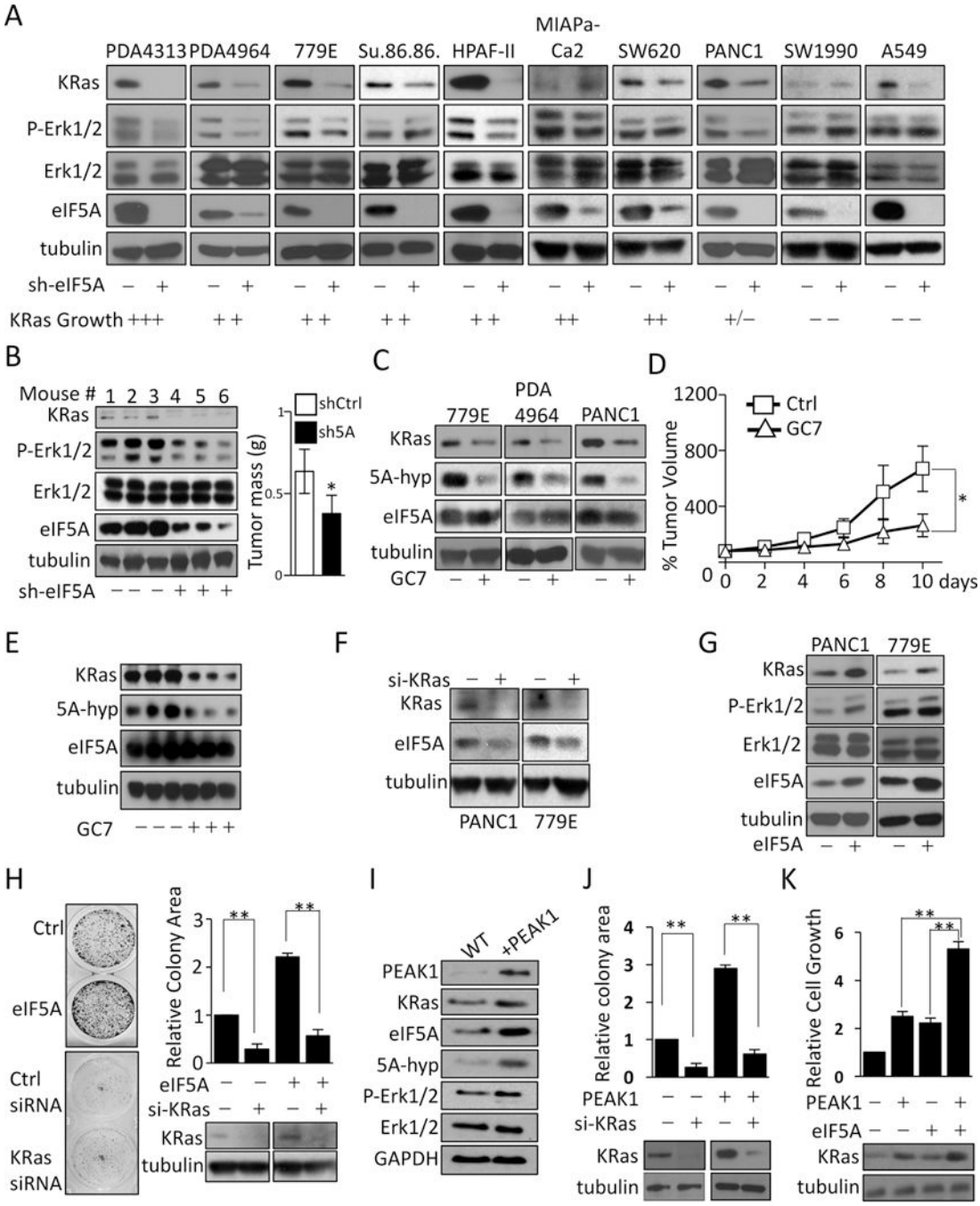


**Figure 1.**

eIF5A-PEAK1 signaling regulates KRAS protein expression. **A**, eIF5A-PEAK1 regulates KRas protein expression. The indicated cancer cells stably expressing lentiviruses encoding control shRNA (−) or shRNA to eIF5A (sh-eIF5A) were western blotted (WB) for the indicated proteins. P-Erk1/2 = phosphorylated activated Erk 1 and 2 kinases. + = relative dependency or on KRas for cell growth. +/− = moderate dependency on KRas for cell growth. − = independent of KRas for cell growth. **B**, Syngeneic orthotopic tumor growth of PDA4964 cells in B6/129 mice expressing control or eIF5A shRNA (sh5A). Tumors were

resected at two weeks, weighed, and WB for the indicated proteins as in A. **C**, The indicated cells were treated with 20 μM GC7 for 48 hours and then WB for the indicated proteins. 5A-hyp = hypusinated/activated form of eIF5A. **D**, 779E human PDAC subcutaneous tumors were allowed to grow for 10 days in nude mice then treated with vehicle (Ctrl, PBS, n=7) or GC7 (25 mg/kg daily, n=8). Tumor volume was measured with a digital caliper. **E**, Tumors from D were excised and WB for the indicated proteins. **F**, The indicated PDAC cells were treated with siRNA to KRas or control siRNAs (−) and WB for the indicated proteins. **G**, The indicated PDAC cells were infected with a lentivirus encoding eIF5A and WB for the indicated proteins. **H**, siRNA-mediated KRas knockdown in 779E cells treated as in G and examined for colony growth *in vitro* and WB for the indicated proteins. Results are relative to control siRNA cells. Inset = picture of colonies stained with crystal violet. **I**, 779E cells stably expressing lentiviruses encoding PEAK1 or control vectors and WB for the indicated proteins. **J**, siRNA-mediated KRas knockdown in 779E cells treated as in I and examined for colony growth *in vitro* and WB for the indicated proteins. **K**, 779E cells induced to express eIF5A, PEAK1, or both eIF5A and PEAK1, and examined for cell growth *in vitro*. Results are relative to control cells transfected with empty vectors. * = $P<0.05$, **=$P<0.01$, Student's *t* test.

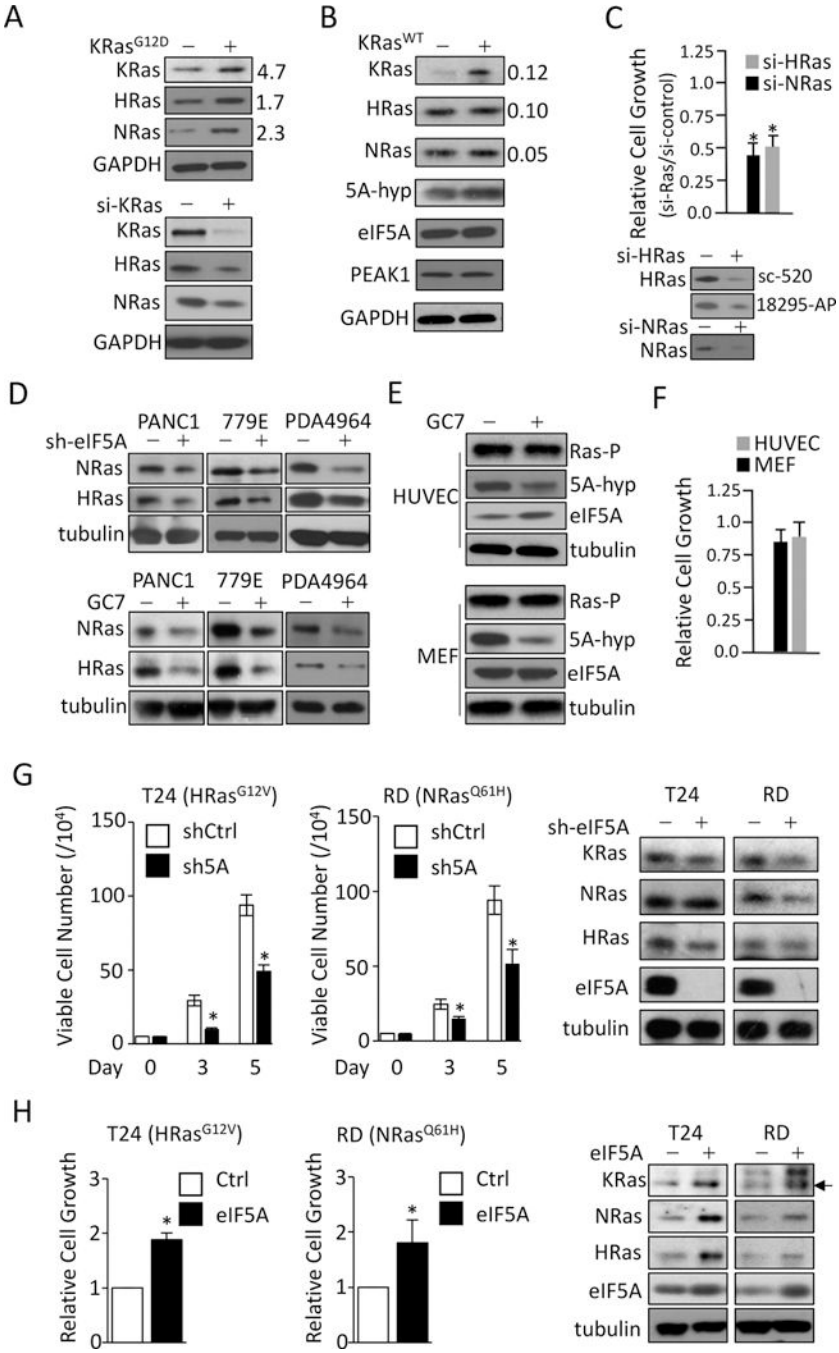


**Figure 2.**

KRas-eIF5A-PEAK1 regulates NRas and HRas protein expression. **A (Upper panel) and B**, HPNE or HPNE cells expressing $KRas^{G12D}$ oncogene or KRas wild type (WT) and WB for the indicated proteins. Numbers show fold increase in GTPase activity (GTP:GDP ratio of $KRas^{G12D+}$/KRas endogenous or $KRas^{WT}$/KRas endogenous) determined using a standard GST-RBD domain pull-down assay. **Lower panel** of A, siRNA-mediated KRas knockdown in HPNE cells expressing $KRas^{G12D}$ and WB for the indicated proteins. **C**, siRNA HRas or NRas knockdown in HPNE-$KRas^{G12D}$ cells and examined for cell growth *in vitro* and WB

for the indicated proteins. HRas was detected with two different antibodies, sc-520, and 18295-AP. **D, Upper panel**, the indicated PDAC cells stably express lentiviruses encoding control shRNA (−) or shRNA to eIF5A (sh-eIF5A) and WB for the indicated proteins. **Lower panel**, the indicated cells were treated with 20 μM GC7 for 48 hours and then WB for the indicated proteins. **E and F**, Human umbilical vein cells (HUVEC) or mouse embryonic fibroblast cells (MEFs) were treated with or without GC7 (20 μM) for 48 hrs and WB for the indicated proteins or examined for cell growth. Results are GC7 treated cell relative to vehicle control. Ras-P was detected with a pan Ras antibody. **G**, The indicated cancer cells stably express lentiviruses encoding control shRNA (shCtrl, -) or shRNA to eIF5A (sh-5A, sh-eIF5A) were examined for changes in viable cell numbers for 0–5 days and WB for the indicated proteins. **H**, The indicated cancer cells were transfected with control vector or eIF5A and examined for cell growth after 5 days and WB for the indicated proteins. Results shown are relative to control vector. Arrow = KRas. * = $P<0.05$, **=$P<0.01$ Student's *t* test.

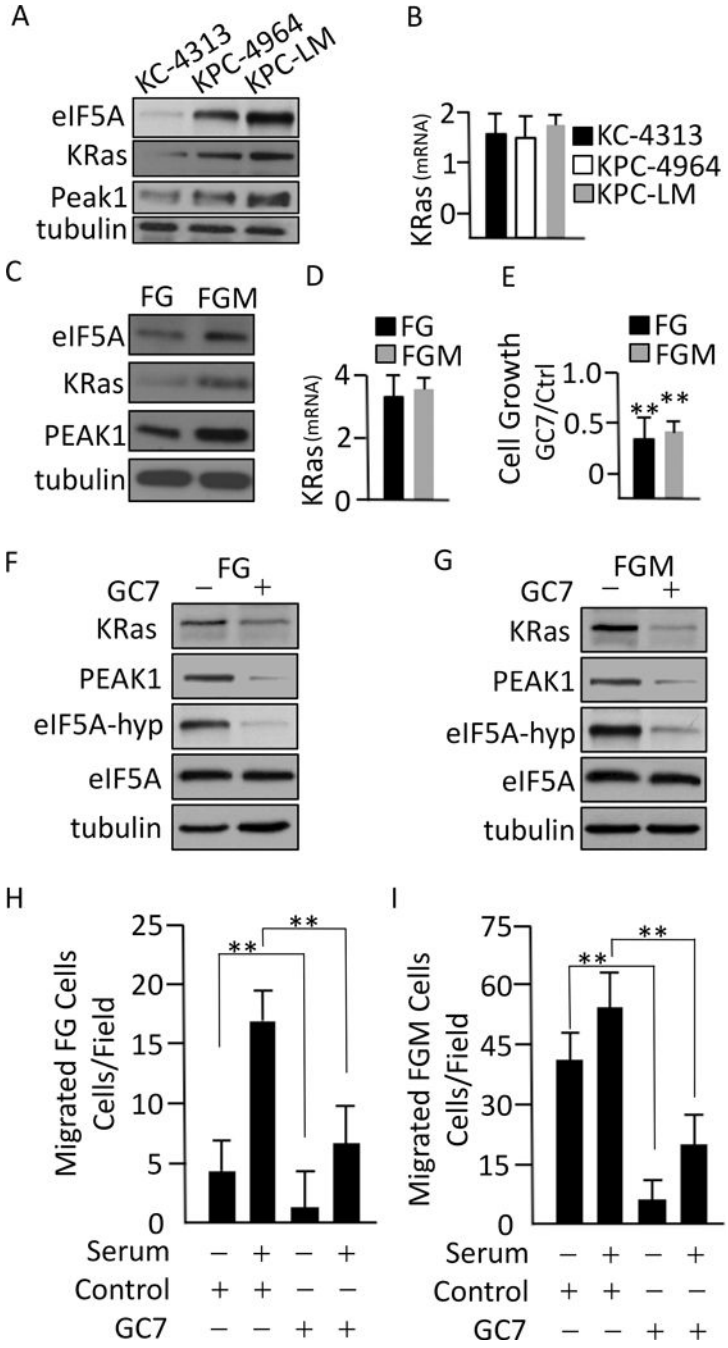


**Figure 3.**

Increased eIF5A, KRas, and PEAK1 protein expression correlated with increased metastatic potential of PDAC cells. **A**, Mouse PDAC cell lines were derived from a PanIN stage KC mouse tumor (KC-PanIN), a primary tumor from KPC mice (KPC-P), or a matched spontaneous liver metastatic nodule from KPC-P mice (KPC-LM) and then WB for the indicated proteins; **B**, KRas mRNA levels relative to GAPDH mRNA levels were determined by qPCR in three independent experiments. No statistical differences were observed in the average KRas mRNA levels in the different cell lines. **C**, Human PDAC low

metastatic (FG cells) or a matched highly migratory/metastatic variant cell lined derived from parental FG cells (FGM) were WB for the indicated proteins. **D**, KRas mRNA levels relative to GAPDH mRNA levels were determined by qPCR in three independent experiments. **E**, Relative cell growth of FG and FGM treated with 20 μM GC7 or control vehicle (Ctrl) for 72 hours cells. **F and G**, Cells treated as in E and WB for the indicated proteins. **H and I**, FG and FGM cells were treated with 20 μM GC7 or control vehicle for 24 hours and then allowed to migrate for 6 hours. * = $P<0.05$, **=$P<0.01$ Student's *t* test.

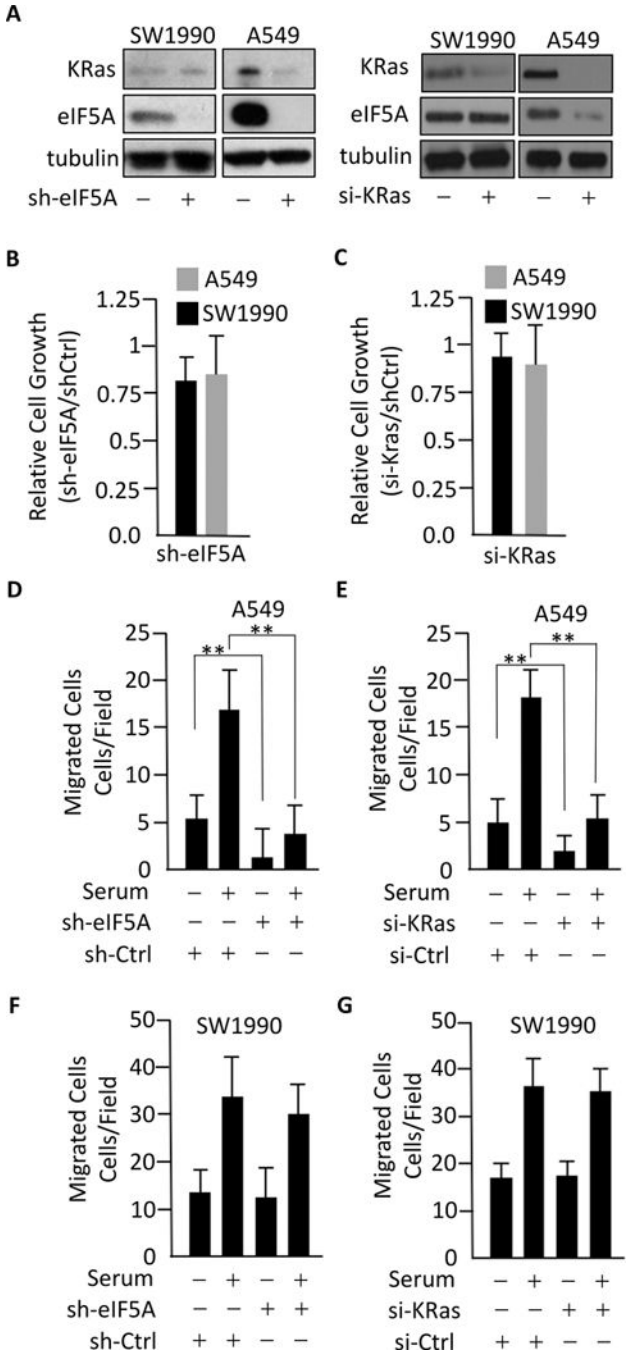


**Figure 4.**

eIF5A controls KRas expression to drive A549 cell migration, but not proliferation. **A**, The indicated cell lines were treated with shRNA to eIF5A, siRNA to KRas, or control siRNAs/shRNA (−) and WB for the indicated proteins. Relative cell proliferation **B and C**, and migration **D-G**, in the presence or absence of chemoattractant (serum) were determine in KRas and eIF5A-depleted cells from A. * = $P<0.05$, **=$P<0.01$ Student's *t* test.

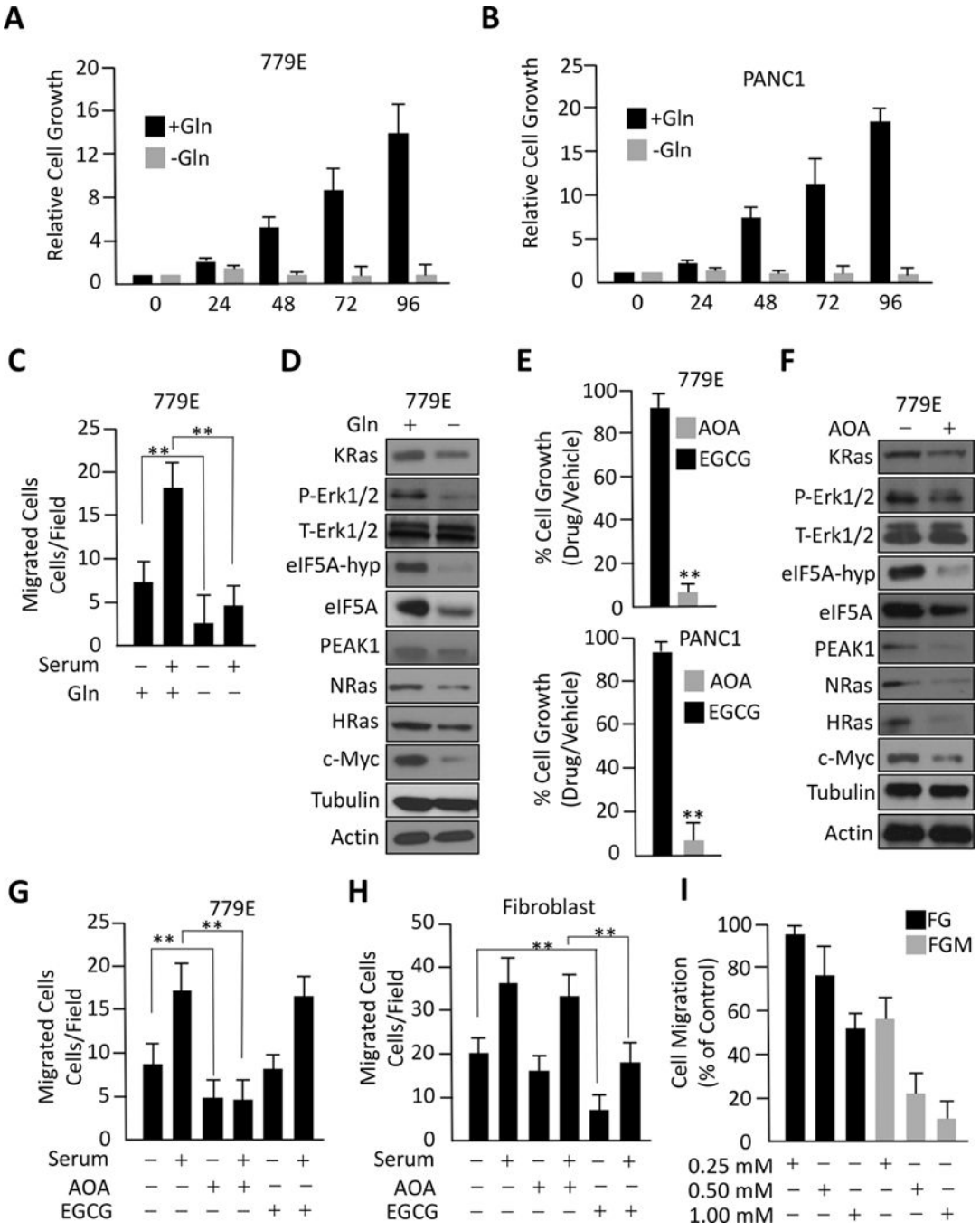


**Figure 5.**

Glutamine deprivation or blocking glutamine metabolism inhibits the KRas-eIF5A-PEAK1 signaling loop, which inhibits PDAC cell proliferation and migration. **A and B**, Relative cell growth in complete media with or without glutamine (Gln) was determined for the indicated days. **C**, 779E cells were grown in complete media with or without glutamine for 72 hours then examined for cell migration for 8 hours in the presence or absence of chemoattractant (serum). **D**, Cells were grown in complete media with or without glutamine for 72 hours then WB for the indicated proteins. **E**, Relative cell growth of PANC1 (upper bar graph) and

779E cells (lower panel) treated with either 1.0 mM AOA (aminooxyacetate) or 100 μM EGCG (epigallocatechin gallate) for 72 hours. **F**, 779E cells treated with AOA as in E and WB for the indicated proteins. **G and H**, 779E PDAC cells and normal human fibroblasts were treated with AOA or EGCG as in D and examined for cell migration for 8 hours in the presence or absence of chemoattractant (serum). **I**, FG and FGM cells were treated with the indicated concentrations of AOA for 72 hours and migration determined for 6 hours. Results are relative to vehicle treated cells. * = $P<0.05$, **=$P<0.01$ Student's *t* test.

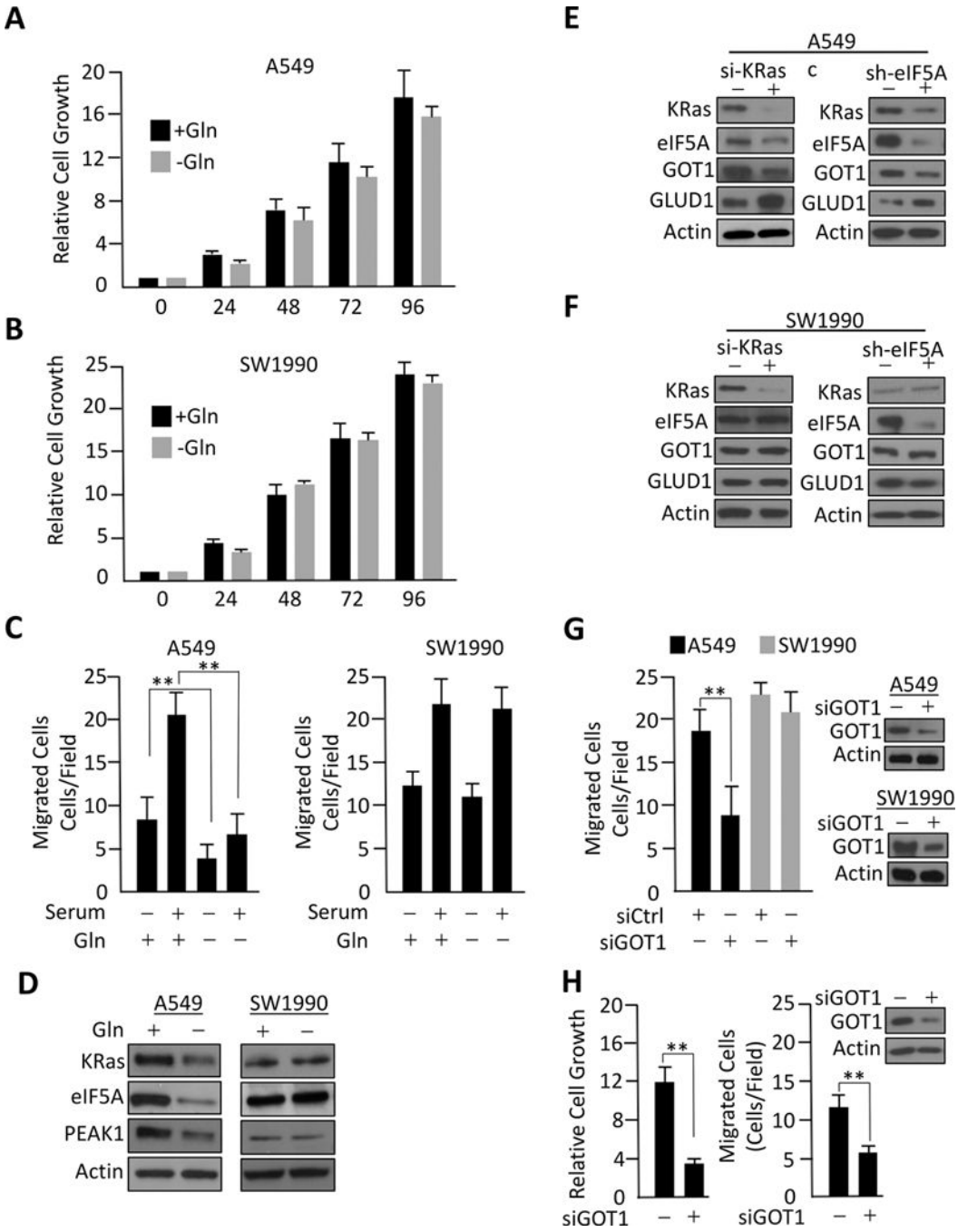


**Figure 6.**

Glutamine deprivation or GOT1 depletion inhibits A549 cell migration, but not cell proliferation. **A and B**, Relative cell growth in complete media with or without glutamine (Gln) was determined for the indicated days. **C**, The indicated cells were grown in complete media with or without glutamine for 72 hours then examined for cell migration for 6 hours in the presence or absence of chemoattractant (serum). **D**, The indicated cells treated as in C and WB for the indicated proteins. **E and F**, The indicated cells were treated with siRNA to KRas, shRNA to eIF5A, or control siRNAs/shRNAs (−) and WB for the indicated proteins.

**G**, The indicated cells were treated with siRNA to GOT1, or control siRNAs (−) and the number of migrating cells determined after 6 hours. Inset shows WB of the indicated proteins from the same cells used for the migration experiments. **H**, 779E cells were treated with siRNA to GOT1, or control siRNAs (−) and relative cell growth for 72 hours or the number of migrating cells after 6 hours determined. Inset shows WB of the indicated proteins from the same cells used for the growth and migration experiments. * = $P<0.05$, **=$P<0.01$ Student's *t* test.

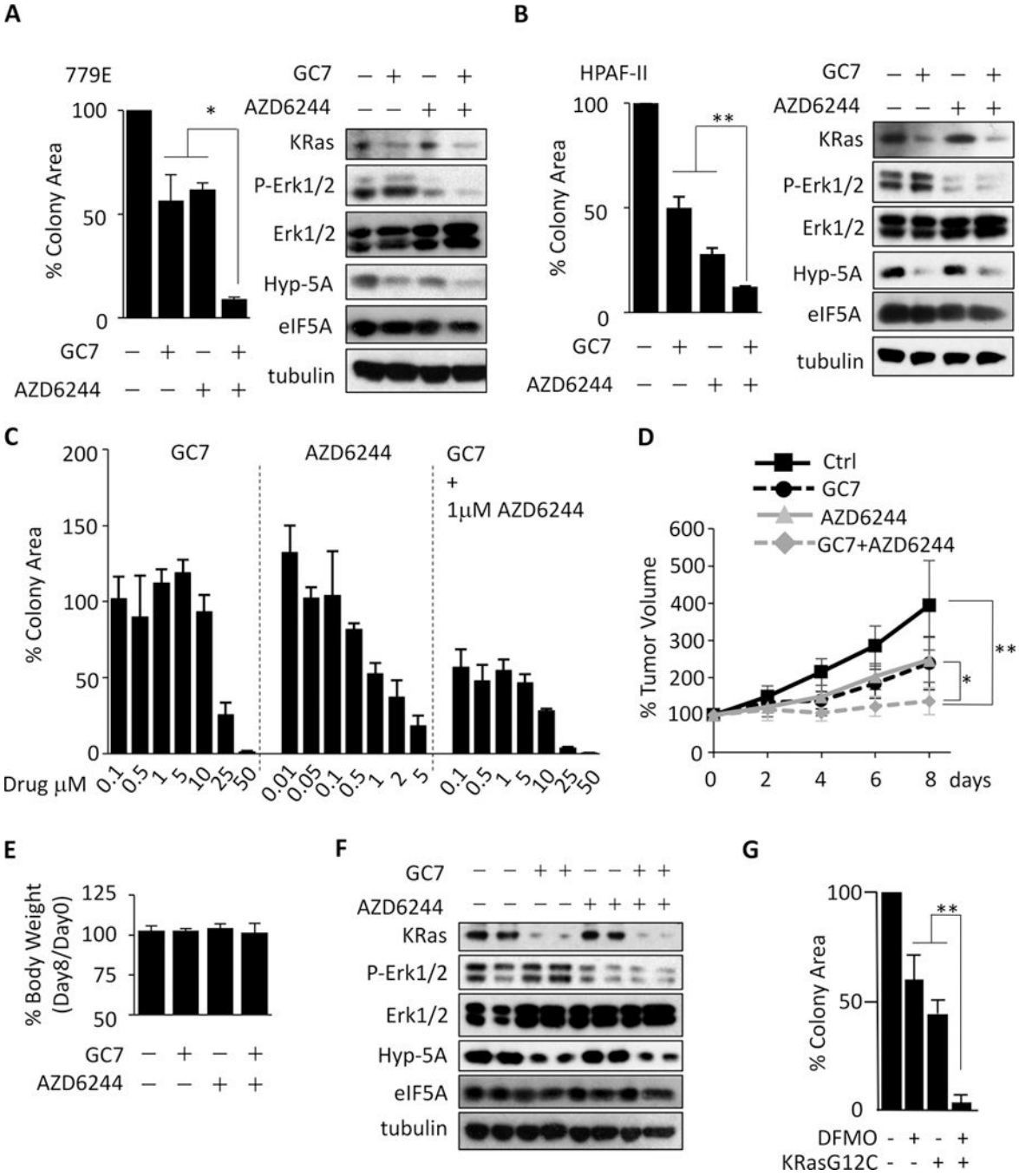


**Figure 7.**

Pharmacological inhibition of eIF5A hypusination sensitizes KRas-driven tumor cells to MEK and KRas inhibition. **A**, 779E cells were treated with the indicated concentration of GC7 and/or AZD6244 for 7 days and cell colonies stained with crystal violet. Bar graph (left) shows stained colony area as measured by ImageJ relative to vehicle control. WB blot (right) was performed from treated cells for the indicated proteins. **B**, HPAF-II cells were treated with GC7 (20 μM) and AZD6244 (1 μM) and subjected to the colony growth assay and WB as in A. **C**, 779E cells were treated with GC7 or AZD6244 alone or in combination

with the indicated drug concentrations and allowed to grow for 7 days. Cell colony area was assessed as in A. **D**, Nude mice subcutaneously implanted with 779E cells were treated with vehicle, GC7, AZD6244 or GC7 and AZD6244 for 8 days and tumor size was measured every other day (bar graph). **E**, The relative body weights of mice treated with drugs as in D. **F**, Lysates from tumors in D were WB for the indicated proteins. **G**, H1792cells were treated with DFMO (0.5 mM) or K-RasG12C compound 12 alone (0.5 μM) or in combination and allowed to grow for 4 days. Cell colony area was assessed as in A. WB of drug treated cells shown in sFig. 5E. * = $P<0.05$, **=$P<0.01$ Student's *t* test.